Photosynthesis Research
https://doi.org/10.1007/s11120-019-00659-0

ORIGINAL ARTICLE

CO_2 uptake and chlorophyll *a* fluorescence of *Suaeda fruticosa* grown under diurnal rhythm and after transfer to continuous dark

Silas Wungrampha[1] · Rohit Joshi[1] · Ray S. Rathore[2] · Sneh L. Singla-Pareek[2] · Govindjee[3] · Ashwani Pareek[1]

Received: 14 May 2019 / Accepted: 4 July 2019

Abstract

Although only 2–4% of absorbed light is emitted as chlorophyll (Chl) *a* fluorescence, its measurement provides valuable information on photosynthesis of the plant, particularly of Photosystem II (PSII) and Photosystem I (PSI). In this paper, we have examined photosynthetic parameters of *Suaeda fruticosa* L. (family: Amaranthaceae), surviving under extreme xero-halophytic conditions, as influenced by diurnal rhythm or continuous dark condition. We report here CO_2 gas exchange and the kinetics of Chl *a* fluorescence of *S. fruticosa*, made every 3 hours (hrs) for 3 days, using a portable infra-red gas analyzer and a Handy PEA fluorimeter. Our measurements on CO_2 gas exchange show the maximum rate of photosynthesis to be at 08:00 hrs under diurnal condition and at 05:00 hrs under continuous dark. From the OJIP phase of Chl *a* fluorescence transient, we have inferred that the maximum quantum yield of PSII photochemistry must have increased during the night under diurnal rhythm, and between 11:00 and 17:00 hrs under constant dark. Overall, our study has revealed novel insights into how photosynthetic reactions are affected by the photoperiodic cycles in *S. fruticosa* under high salinity. This study has further revealed a unique strategy operating in this xero-halophyte where the repair mechanism for damaged PSII operates during the dark, which, we suggest, contributes to its ecological adaptation and ability to survive and reproduce under extreme saline, high light, and drought conditions. We expect these investigations to help in identifying key genes and pathways for raising crops for saline and dry areas.

Keywords Chlorophyll · Diurnal rhythm · Fluorescence · JIP test · Photoinhibition · Salinity

Abbreviations

Chl	Chlorophyll
C_i	Internal CO_2 concentration
EC	Electrical conductivity
ETR	Electron transport rate
F_v/F_m	Maximum quantum yield of Photosystem II (PSII)
G_s	Stomatal conductance
hrs	hours
NPQ	Non-photochemical quenching of the excited state of Chl, usually by heat loss
NPR	Net photosynthesis rate
q_N	A coefficient for non-photochemical quenching of the excited state of Chl
q_P	A coefficient for photochemical quenching of the excited state of Chl
ROS	Reactive oxygen species
T_r	Transpiration rate

Electronic supplementary material The online version of this article (https://doi.org/10.1007/s11120-019-00659-0) contains supplementary material, which is available to authorized users.

✉ Ashwani Pareek
ashwanip@mail.jnu.ac.in

[1] Stress Physiology and Molecular Biology Laboratory, School of Life Sciences, Jawaharlal Nehru University, New Delhi, India

[2] Plant Stress Biology, International Centre for Genetic Engineering and Biotechnology, Aruna Asaf Ali Marg, New Delhi, India

[3] Department of Biochemistry, Department of Plant Biology, and Center of Biophysics and Quantitative Biology, University of Illinois at Urbana-Champaign, Urbana, IL 61801, USA

Introduction

Salinity stress, irrespective of plant's developmental stage, leads to severe reduction in plant growth, development, as well as yield (Joshi et al. 2016; Kumar et al. 2012; Pareek et al. 2010; Wungrampha et al. 2018). Salinity affects the whole plant architecture causing reduction in leaf area,

Published online: 17 July 2019

which further limits light interception by the canopy, stomatal diffusion, and photosynthetic rate (Chen et al. 2017). It is well established that high level of salinity primarily targets photosynthesis by impairing the photochemical efficiency of both Photosystem I (PSI) and Photosystem II (PSII), by reducing their overall maximum quantum yield, the rate of electron transport, and the overall performance index (Allakhverdiev et al. 2000; Kan et al. 2017; Soda et al. 2018). High salinity also causes swelling and degradation of thylakoids and impairs granal stacking as well as chloroplast envelope development; further, it increases the number of plastoglobuli. In general, all these effects are most likely due to the production of reactive oxygen species (ROS), which lead to ultrastructural damage of the chloroplasts, as has been shown in several plants (Bastías et al. 2015; Meng et al. 2016). Although plants are sessile, they are able to deal with sublethal levels of several abiotic stresses (such as salinity, low temperatures, oxidative stress) as well as daily fluctuations in photosynthesis (due to changes in light intensity) by relying on and utilizing circadian oscillators (Bendix et al. 2015; Sharan et al. 2017; Shor and Green 2016; Webb 2003). Light intensities, as well as the duration of light and dark cycles (photoperiodic length), play a crucial role in the growth and development of plants (McClung 2006; Schaffer et al. 2001). This photoperiodic entrainment modulates the physiological harmony of the plant such as its growth, stomatal opening, leaf movement, and molecular responses by regulating the expression of certain genes at particular times (McClung 2006; Schaffer et al. 2001; Singh et al. 2015). Two parameters that modulate the photoperiod cycle of an organism are diurnal and circadian rhythm. The endogenous cycle/rhythm that occurs within a period of 24 hrs is called circadian. However, the oscillating rhythm that is synchronized by day/night cycle is diurnal rhythm (see, e.g., Soni et al. 2013; Webb 2003). There are two principal factors that govern diurnal rhythm in plants: the internal oscillating clock, the circadian clock (circadian rhythm), and light (De Caluwé et al. 2017; Schaffer et al. 2001). Endogenous circadian oscillators occur in all organisms which act as autoregulatory feedback loops driving the rhythmic behavior of genes, proteins, and metabolites (De Caluwé et al. 2017). In plants, the photoperiodic entrainment of environmental cues is 'gating' of the response to a stimulus through rhythmic synchronization of transcriptional, translational, and post-translational modulations of large gene families. These genes, in turn, regulate plant growth and development by activating and accumulating stress-responsive proteins and metabolites (Greenham and McClung 2015). The fine-tuning responses are brought in by "alternative splicing," controlled protein turnover, and chromatin modifications, which allow the plants to coordinate their temporal organization of biological processes with daily and seasonal changes with light and temperature cycles (Greenham and McClung 2015; Mora-García et al. 2017). Both the internal state of the plant and the external environment influence the "pulse" of the oscillator clock by regulating the expression of its components. Successively, the clock ensures the activation of certain genes regulating multitude of metabolic and physiological aspects of plants that are suitable, during day or night, in providing fitness advantage in developmental processes during the life cycle of a plant (Cano-Ramirez and Dodd 2018; De Caluwé et al. 2017; Dodd et al. 2014).

We know that the pattern of changes in photosynthesis and respiration is influenced by diurnal rhythm in various plants including oak-grass savanna species (Tang et al. 2005), *Quercus palustris* (Epron et al. 1992), *Glycine max* (Zhang et al. 2007), *Zea mays* (Leakey et al. 2004), *Vitis vinifera* (Downton et al. 1987), grassland species (Bahn et al. 2009), and Chinese flowering *Castanea* sp. (Cheng et al. 2016). Further, under stress, regulation of photosynthetic machinery is influenced by diurnal rhythm in plants such as *Solanum lycopersicum* (Ikkonen et al. 2015), *Hordeum vulgare* (Goldstein et al. 2017), *Oryza sativa* (Kim et al. 2017; Singh et al. 2015), *Z. mays* (Feng et al. 2017), *G. max* (Pan et al. 2015), *Arabidopsis thaliana* (Nitschke et al. 2016), and *Gossypium* sp. (García-Plazaola et 2017).

Unlike the glycophytes, halophytes have acquired certain photoprotective mechanisms since they have 'superior' alleles of the genes (involved in ion homeostasis, or production of osmoprotective compounds or anti-oxidative enzymes) for avoiding photodamage under high salinity (Sengupta et al. 2018). *Suaeda fruticosa*, used in our study, is a xero-halophyte well adapted to extreme desert environments and high saline conditions; it does it by maintaining high chlorophyll (Chl) *a*/*b* ratio and by accumulating osmoprotectants, such as proline and sugars (Flowers and Colmer 2015; Ullah and Bano 2015). However, no study has, thus far, been carried out to investigate the photoperiodic control of photosynthesis in this plant. Thus, the aim of our study was to understand the complex machinery associated with photosynthesis under diurnal rhythm conferring adaptive advantage to this plant by measuring the CO_2 gas exchange and Chl *a* fluorescence. These provide us information on the basic photosynthetic efficiency of *S. fruticosa* surviving under xerophytic conditions (Mishra et al. 2016). To further test if eliminating light in *S. fruticosa* by keeping it under continuous dark affects CO_2 and H_2O fluxes, we maintained the plants under diurnal rhythm initially for 24 hrs, and then kept them under complete darkness for 48 hrs, under their natural habitat.

In this paper, we have systematically studied the entrainment capability of *S. fruticosa* at different photoperiods of the light–dark cycle in order to analyze the influence of diurnal rhythm and of continuous dark on PSII efficiency. This was done by measuring changes in the maximum quantum yield of PSII photochemistry [via changes in the ratio of the

variable (F_v) to maximal (F_m) Chl fluorescence]. Additionally, we measured the overall photosynthesis performance index at dawn and at dusk under both diurnal and continuous dark conditions. Our investigation provides a comprehensive analysis of PSII photochemistry, photoinhibition, and photoprotection in *S. fruticosa* under extreme saline conditions. Furthermore, the dynamic behavior of the photosynthetic machinery observed, in this study, under diurnal condition confirms the contribution of the photoperiodic entrainment in providing tolerance against the saline environment in xero-halophytes.

Materials and methods

Plant material and growth conditions

We conducted our study at the Sambhar Salt Lake (India's largest inland playa within the Thar Desert) located in the middle of the Aravalli schists, India (26°58′N, and 75°5′E), where *S. fruticosa* population is high. The average temperature of this area reaches up to 50 °C during the summers and goes down to as low as 3 °C during the winters, with a total salinity of 45–50 dS m^{-1} and the pH range of 8.4–10.5 throughout the year (Krishna et al. 2014; Roy and Singhvi 2016). Sambhar Lake receives an annual rainfall of 100–500 mm, mostly during the monsoon season (Sinha and Raymahashay 2004). At the site of our research, light intensity was measured from ~ 05:00 to ~ 20:00 hrs, before and after which the light intensity was reduced to nearly zero (to provide darkness). The maximum photosynthetically active radiation (PAR) on a clear day was 1800 µmol photons m^{-2} s^{-1}, as measured by LX-101A Lux Meter (HTC Instruments, India) between 10:00 and 15:00 hrs (Supplementary Fig. S1). The plants that were monitored under continuous dark had been covered with a double-layered thick dark cloth, which had only ~ 1% transmission of the day light (Supplementary Fig. S2), from 300 to 900 nm, as measured by a Cary 300 UV–visible spectrophotometer (Agilent, USA).

Gas exchange measurements

Leaf gas exchange parameters for *S. fruticosa*, under diurnal and continuous dark, were recorded using a Li-6400XT (Li-Cor, Inc., Lincoln, USA) portable infra-red gas analyzer (IRGA). Measurements were made continuously for 72 hrs at 3 hr intervals on plants kept under both the experimental conditions (see above); in these experiments, at least 2/3 of the IRGA chamber area was covered with leaves of *S. fruticosa*. For the case of continuous dark, the first 24 hrs of the experiment was under diurnal condition, and then, for the next 48 hrs the plant was covered with two layers of the black cloth (cf. Kolosova et al. 2001). However, all other conditions were maintained similar to those used for plants under diurnal condition. In order to measure transpiration rate (T_r), stomatal conductance (G_s), net photosynthetic rate (NPR), and intercellular CO_2 mol fraction (C_i) under in situ conditions, we measured them at ambient CO_2 concentration (400 µmol mol^{-1}) and at photosynthetic photon flux density (PPFD) of 2900 µmol photons m^{-2} s^{-1}, obtained from the blue and the red light emitting diodes.

Measurement of chlorophyll *a* fluorescence

Chlorophyll a fluorescence kinetics were measured with Handy PEA-plant efficiency analyzer (Hansatech Instruments, King's Lynn, Norfolk, UK) instrument. The parameter for non-photochemical quenching (NPQ) of the excited state of Chl *a*, the coefficient for photochemical quenching (q_P), the coefficient for non-photochemical quenching (q_N), and the total electron transport rate (ETR) through PSII were calculated as follows (see, e.g., Lazár 2015): (1) $NPQ = (F_m - F'_m)/F'_m$, where F_m is the maximum Chl fluorescence in dark-adapted plants, and F'_m is the maximum Chl fluorescence in light-adapted plants, which is a measure of the excitation energy dissipation in PSII antenna, (2) $q_P = (F'_m - F(t))/(F'_m - F'_o)$, where $F(t)$ is the Chl fluorescence measured at time t, which indicates the proportion of open PSIIs (i.e., with Q_A in the oxidized state). (3) $q_N = ((F_m - F_o) - (F'_m - F'_o))/(F_m - F_o)$, which is a coefficient for non-photochemical quenching that requires measurement of the initial fluorescence of the dark-adapted and light-adapted sample (i.e., F_o and F'_o), and (4) $ETR \approx \Phi_{PSII} \cdot PPFD \cdot A \cdot 0.5$, where $\Phi_{PSII} = (F'_m - F_s)/F'_m$ is the light-adapted quantum yield of PSII, F_s being the Chl fluorescence of the light-adapted sample, and PPFD (photosynthetically active photon flux density) being the incident irradiance, A the leaf absorbance (estimated as 0.84), and 0.5 is for the assumed equal distribution of photons between PSI and PSII. In addition, the variable-to-maximum fluorescence ratio, F_v $(= F_m - F_o)/F_m$, was measured on dark-adapted (10 min) leaves of *S. fruticosa*, by Handy PEA-plant efficiency analyzer (Hansatech Instruments Ltd., Petney, Norfolk, UK). Measurements were made for 72 hrs at every 3 hrs.

The Chl *a* florescence induction transient of the dark-adapted samples was measured with a 300 s 650 nm excitation light of several intensities between 2500 and 3400 µmol photons m^{-2} s^{-1}, to find the light intensity at which the "P" level reaches the maximal fluorescence (F_m); our results showed that in our samples, F_m is reached when the excitation light intensity is 2900 µmol photons m^{-2} s^{-1} (see Supplementary Fig. S3). For measurement of OJIP, 1–2 s are used; however, to include SMT phase, we measured Chl fluorescence up to 300 s (Stirbet et al. 2018). Here, no

maxima was detected in the SMT phase region; therefore, it is not discussed in this paper. Further, the readings obtained from the Handy PEA were double normalized at F_o and at F_m by using the PEA Plus software (version 1.12), and analyzed by using the so-called JIP-test, which is based on the general concepts of energy fluxes in bio-membranes (see Strasser 1978; Strasser et al. 2004). The following energy fluxes were defined in the JIP test: photon absorption by PSII antenna (ABS), trapping of excitation energy flux by the PSII reaction center (TR_o), dissipation of the excitation energy flux in PSII antenna (DI_o, which equals $ABS - TR_o$), electron transport (ET_o) from PSII to the plastoquinone (PQ) pool, and reduction of the end (electron) acceptors of PSI (RE_o). The Chl *a* fluorescence transient was plotted on a logarithmic time scale to be able to see clearly all the steps of the "OJIP" phase; further, Chl *a* fluorescence at 50 µs was taken as the minimum fluorescence (F_o). Using the measured fluorescence data sets, we have calculated several JIP parameters (see Table 1 for the abbreviations, definitions and equations), as presented by Stirbet and Govindjee (2011) and Stirbet et al. (2018).

Statistical analysis

Measurements of Chl *a* fluorescence as well as of gas exchange were statistically analyzed using ANOVA model (Fisher 2006). Only measurements having significant values ($p < 0.05$) are shown in the figures. For each time point, six replicate readings were taken for both diurnal and continuous dark experiments. From this, a heat map was developed using Multi Experiment Viewer (MeV) version 4.9 to visualize the values of the JIP parameters used in the analysis (Saeed et al. 2006). This heat map was generated by normalizing the values and bringing them all to a range between 1 and 100% to provide an unbiased color code. Three color code combination of red for high (100%), yellow for medium (50%), and green for the lowest value (1%) was used to represent the heat map. Percentage values generated after normalization are tabulated in Supplementary Tables 1 and 2.

Results

Leaf gas exchange and fluorescence measurements under diurnal and continuous dark conditions

The leaf gas exchange of *S. fruticosa* was measured under in situ conditions for the plants under diurnal as well as under continuous dark condition at 3-hr intervals for 72 hrs (as described in "Materials and methods" section). Clear rhythmic activity was observed in all the photosynthetic parameters in this study, repeated every 24 hrs (Figs. 1, 2). Plants kept under continuous dark showed damping in the gas exchange values under dark conditions (right panel of Figs. 1, 2). However, parameters such as F_v/F_m, NPR, ETR, and T_r (Fig. 1) showed noticeable rhythm even under dark conditions (though the amplitudes were smaller than under diurnal rhythm). The parameters that noticeably changed under continuous dark condition are shown in Fig. 1, while the parameters that did not exhibit any noticeable change under continuous dark, as compared to changes observed under diurnal condition are, presented in Fig. 2. The weak fluctuation in photosynthetic parameters, observed in *S. fruticosa*, kept under continuous dark, is shown in Supplementary Fig. S5, after separating observations from two datasets (i.e., diurnal for the first 24 hrs, and continuous dark for the next 48 hrs).

The maximum PSII quantum yield, calculated from the Chl *a* fluorescence (i.e., F_v/F_m), showed the highest value at 23:00 hrs, with its high level maintained till dawn under diurnal rhythm. However, under continuous dark, F_v/F_m was high between 08:00 and 17:00 hrs, with its maximum value observed at 14:00 hrs (Fig. 1a, b), while under the diurnal rhythm it had the lowest value during the same period. In contrast to the maximum quantum yield, the NPR and ETR had the highest values at 08:00 hrs and between 08:00 and 14:00 hrs under diurnal conditions (Fig. 1c, d), as well as at 05:00 hrs under continuous dark condition (Fig. 1e, f). Similarly, the transpiration rate (T_r) showed the highest value between 08:00 and 17:00 hrs under diurnal conditions (Fig. 1g), and at 05:00 hrs under continuous dark condition (Fig. 1h). Parameters such as internal CO_2 concentration (C_i), stomatal conductance (G_s), non-photochemical quenching with values between zero and infinity (NPQ), photochemical quenching (q_P) and non-photochemical quenching (q_N), with values ranging from zero to one, showed damping under continuous dark condition, and the fluctuations could not be noticed, as compared to those under diurnal conditions (Fig. 2a–j).

Suaeda fruticosa under continuous dark showed maximum ETR, T_r, C_i, and NPQ at 05:00 hrs, which gradually decreased until the next cycle, which is an opposite response observed under diurnal rhythm, where it showed maximum activities of the same parameter during daytime, i.e., between 08:00 and 17:00 hrs. However, G_s, NPR, q_P, and q_N, under continuous dark, showed almost a similar pattern of activity as under diurnal rhythm (with some minor differences in the time of the peak). However, the amplitudes for all these parameters were strikingly lower under dark than the diurnal setup (Supplementary Figs. S5; 2).

Polyphasic chlorophyll *a* fluorescence rise in *Suaeda fruticosa* under diurnal rhythm and continuous dark

To further determine the influence of the diurnal rhythm and the elimination of light on the function and qualitative

Table 1 Abbreviations, formulas, and definitions of the JIP-test parameters used in the current study (cf. Strasser et al. 2000, 2004)

Technical fluorescence parameter		
t_{Fm}	Total time taken to attain maximum fluorescence	Time to reach F_m
Area	The area between the fluorescence curve and the line $F = F_m$	The total area over the O–J–I–P curve
F_o	F(50 µs)	Minimum fluorescence (fluorescence at 50 µs)
$F_{maximum}$		Maximum fluorescence
V_j	$(F_j - F_o)/(F_m - F_o)$	Relative variable fluorescence at 2 ms
V_i	$(F_i - F_o)/(F_m - F_o)$	Relative variable fluorescence at 30 ms
N	$[\text{Area}/(F_m - F_o)]\cdot M_o\cdot(1/V_j)$	Turnover number: number of Q_A reduction events between time 0 to F_m
M_o	$4\{F_k(0.3\text{ ms}) - F_o\}/(F_m - F_o)]$	Initial slope of the O–J–I–P curve (slope of the O to J rise)
M_{JI}	$\{F(3\text{ ms}) - F(2\text{ ms})\}/(F_m - F_o)$	Slope of the J to I rise
M_{IP}	$0.2\{F(35\text{ ms}) - F(30\text{ ms})\}/(F_m - F_o)]$	Slope of the I to P rise
Specific energy fluxes per active PSII reaction center		
ABS/RC	$(M_o/V_j)/(F_v/F_m)$	Absorbed photon flux by an active PSII reaction center (i.e., the antenna size of an active PSII reaction center)
DI_o/RC	$(ABS/RC) - (TR_o/RC)$	Energy flux dissipated per active PSII reaction center
TR_o/RC	M_o/V_j	Maximal trapped energy flux by a PSII reaction center
ET_o/RC	$M_o\cdot(1/V_j)\cdot(1 - V_j)$	The electron transport flux per active PSII reaction center
Phenomenological energy fluxes defined at F_o		
ABS/CS_o	$\approx F_o$	Absorbed photon flux per excited PSII cross section at time zero
DI_o/CS_o	$(ABS/CS_o) - (TR_o/CS_o)$	Energy flux dissipated per excited PSII cross section at time zero
TR_o/CS_o	$(F_v/F_m)\cdot(ABS/CS_o)$	The maximum trapped exciton flux per excited PSII cross section a time zero
ET_o/CS_o	$(F_v/F_m)\cdot(1 - V_j)\cdot(ABS/CS_o)$	Electron transport flux per excited PSII cross section at time zero
Phenomenological energy fluxes, defined at F_m		
ABS/CS_m	$\approx F_m$	Absorbed photon flux per excited PSII cross section at F_m
DI_o/CS_m	$(ABS/CS_m) - (TR_o/CS_m)$	Energy flux dissipated per excited PSII cross section at F_m
TR_o/CS_m	$(F_v/F_m)\cdot(ABS/CS_m)$	Maximum trapped exciton flux per excited PSII cross section at F_m
ET_o/CS_m	$(F_v/F_m)\cdot(1 - V_j)\cdot(ABS/CS_m)$	Electron transport flux per excited PSII cross section at F_m
Performance index		
PI_{total}	$PI_{total} = PI_{ABS}\cdot(1 - V_i)/(V_i - V_j)$	Performance index showing the conservation of energy from excitation of PSII, until the reduction of the last acceptor molecules of PSI (the complete photochemistry)

For background and reviews on different aspects of the relationship of chlorophyll *a* fluorescence with the photosynthesis, used in our paper, see e.g., Papageorgiou and Govindjee (2004), Schreiber et al. (1986), Stirbet and Govindjee (2012) and Stirbet et al. (2014)

parameters of PSII, we analyzed the OJIP phase of Chl *a* fluorescence transient (Fig. 3). The average fluorescence of *S. fruticosa* from zero to 300 s for each time point for 72 hrs under diurnal rhythm is shown in Fig. 3a, on a logarithmic time scale. The distinct rise (from O to P) in the O–J–I–P fluorescence curve was observed at all the time points measured in both diurnal and continuous dark conditions. However, the O level (F_o) varied throughout

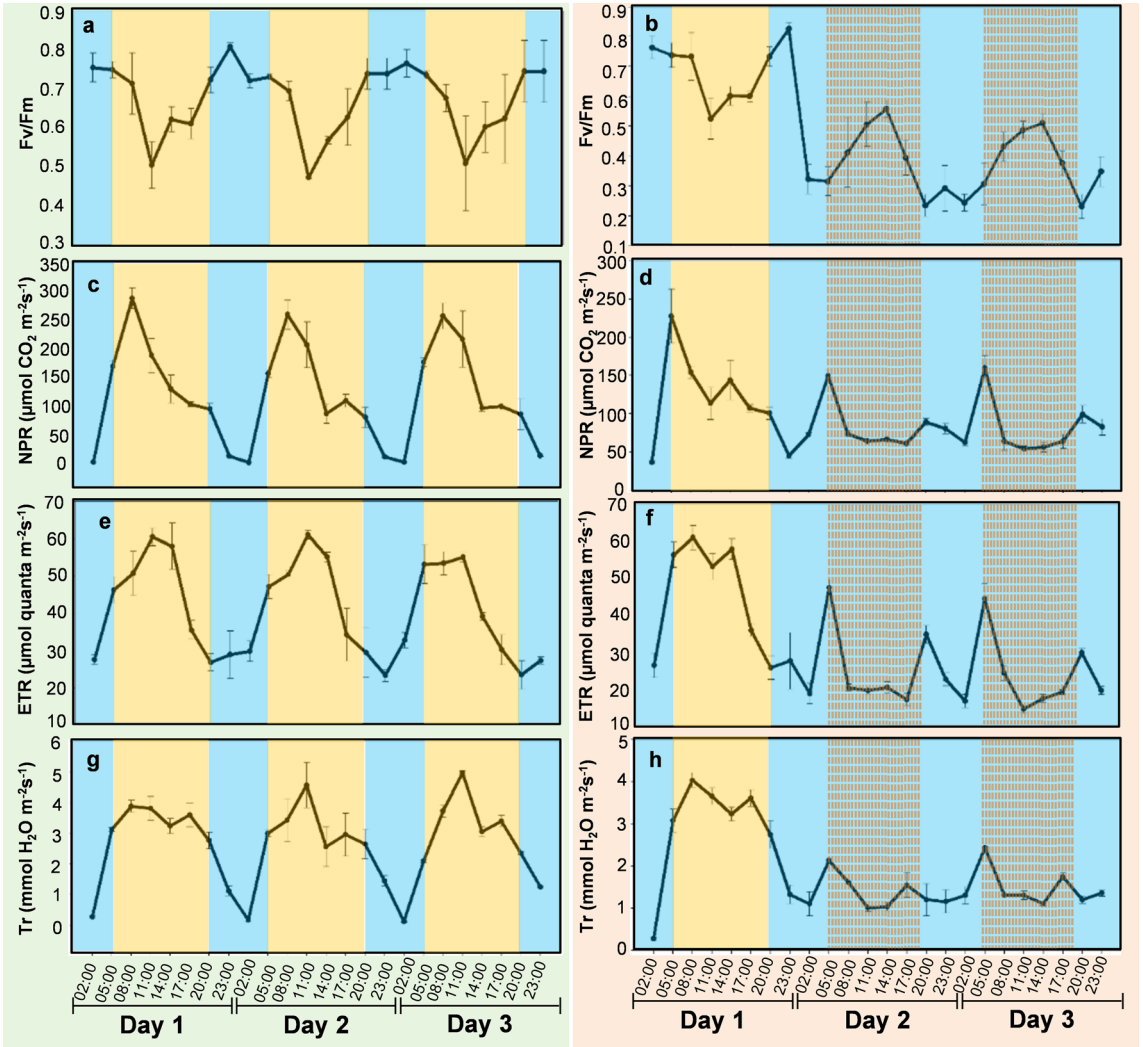

Fig. 1 Photosynthetic parameters for *Suaeda fruticosa* showing noticeable fluctuations in the amplitude under diurnal rhythm and continuous dark; the blue area indicates night, the orange day, and the striped brownish portion indicates continuous dark that was maintained by covering with two layers of black cloth. The right panel shows photosynthesis parameters under continuous dark, where during the first 24 hrs, the plant was kept under diurnal condition, followed by 48 hrs under dark. All parameters, at different time points of the day, were measured on the leaves of *S. fruticosa* for 72 hrs (3 days). A clear rhythmic activity that repeats after every 24 hrs was seen in all the parameters. **a**, **b** Quantum yield of the photosystem II as inferred from the Chl *a* fluorescence, **c**, **d** net photosynthesis rate, **e**, **f** electron transport rate, and **g**, **h** transpiration rate

the day, wherein the minimum value was observed at 14:00 hrs and 11:00 hrs under diurnal, and at 11:00 hrs and 05:00 hrs under continuous dark. The OJIP curve was plotted as F/F_o (i.e., normalized to the "O" level; see calculation in Table 1) to focus on the changes in the OJIP curve. The highest OJIP polyphasic rise was observed at 23:00 hrs, while the minimum fluorescence rise was observed between 14:00 and 17:00 hrs (Fig. 3b). Throughout the day, each time point showed variability in photosynthetic activity as well as in the functional and qualitative parameters of PSII. To further analyze the differences in various photosynthetic parameters, such as the area of the OJIP fluorescence rise, the time to attain F_m, and other parameters represented in Table 1, the measured fluorescence curve was double normalized, i.e., at both F_o and F_m levels, and represented by $V(t) = (F(t) - F_o)/(F_m - F_o)$ (Fig. 3c). This allowed us to focus on observing the rates of changes during the entire OJIP curves, across all the time points. Distinct changes in the OJIP rise and in the parameters, such as the initial slope, the time to reach J, I, and P levels, and the area over the curve, were observed for all the time points under both continuous dark and diurnal conditions. With respect to the J level, two distinct sets of OJIP transient rise were observed under diurnal condition. The time taken to reach J at 11:00, 14:00, 17:00, and 23:00 hrs was shorter than that at 02:00, 05:00, 08:00,

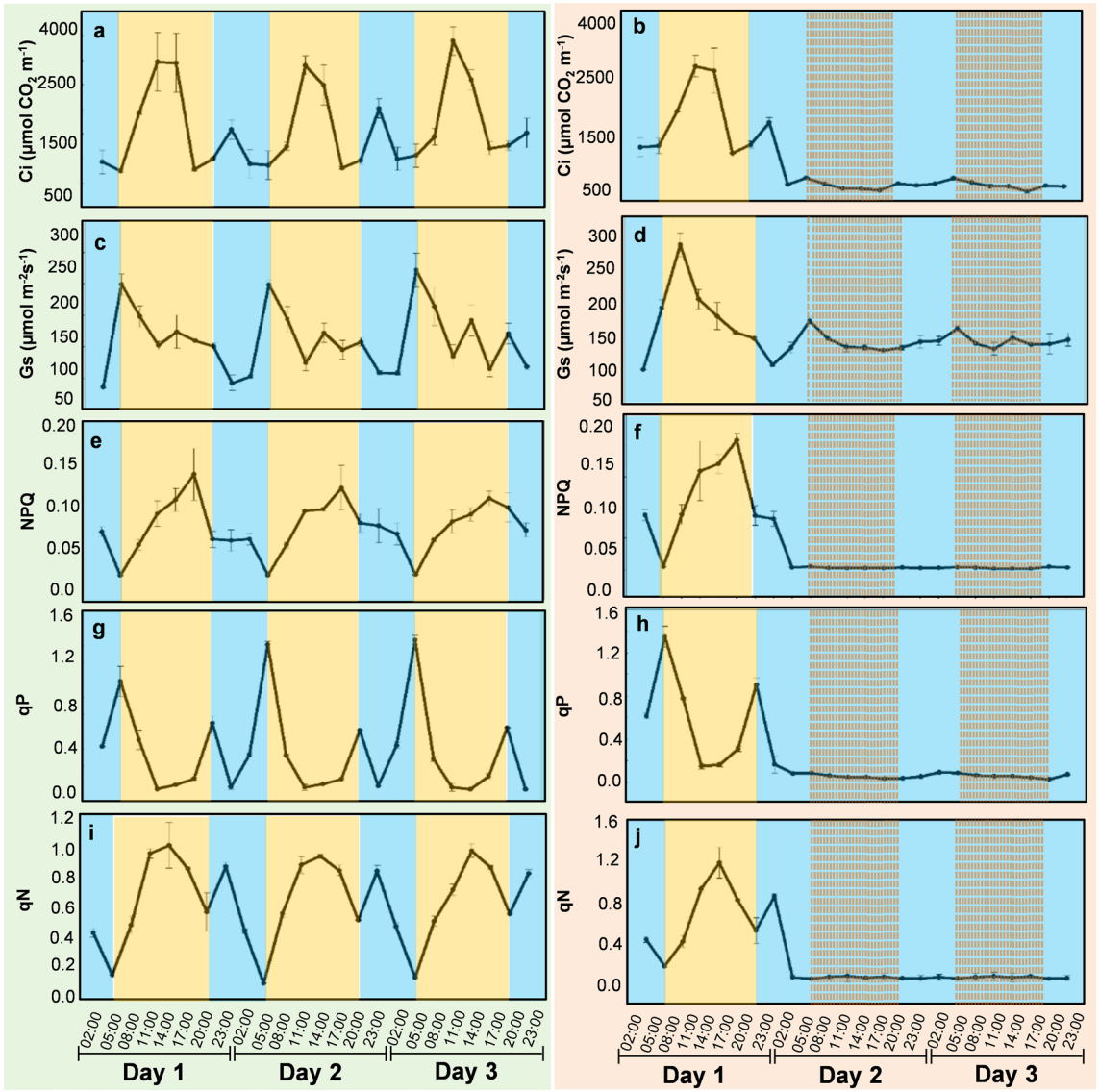

Fig. 2 Photosynthetic parameters for *Suaeda fruticosa* not showing any noticeable fluctuations in the amplitude after maintenance under continuous dark; the blue areas indicate night, the orange day, and the striped brownish portion indicates continuous dark (maintained by covering with a double layer of black cloth). The right panel shows the photosynthesis parameters under continuous dark, where during the first 24 hrs, the plant was maintained under diurnal condition, followed by a 48-hr dark period. Photosynthetic parameters at different time points of the day were measured from the leaves of *S. fruticosa* for 72 hrs (3 days). **a**, **b** Internal CO_2 concentration, **c**, **d** stomatal conductance, **e**, **f** non-photochemical quenching of the excited state of Chl, usually by heat loss, **g**, **h** a quotient for photochemical quenching of the excited state of Chl, and **i**, **j** a quotient for non-photochemical quenching of the excited state of chlorophyll

and 20:00 hrs. However, under continuous dark, such a distinction was not observed.

Similarly, the time-resolved fluorescence induction kinetics of *S. fruticosa* from zero to 300 s for each time point for 48 hrs (excluding the first 24 hrs) under continuous dark, plotted on a logarithmic scale, is shown in Fig. 3d. Further, Fig. 3e shows the curves normalized to F_o (i.e., F/F_o). In contrast to the diurnal rhythm, the typical OJIP polyphasic fluorescence rise under continuous dark was maximum at 11:00 hrs, while the minimum fluorescence rise was observed at 02:00 hrs. The relative variable fluorescence $V(t) = (F(t) - F_o)/(F_m - F_o)$ was calculated and represented at different time points throughout the day at 3-hr intervals under dark conditions. Unlike the plant under diurnal condition, which showed two distinct kinetics of the OJIP fluorescence rise, no such distinct sets were observed under continuous dark condition, but the OJIP kinetics was different at each time point (Fig. 3f).

Quantitative estimation of the PSII activity by analyzing the transient fluorescence rise of *S. fruticosa* under diurnal

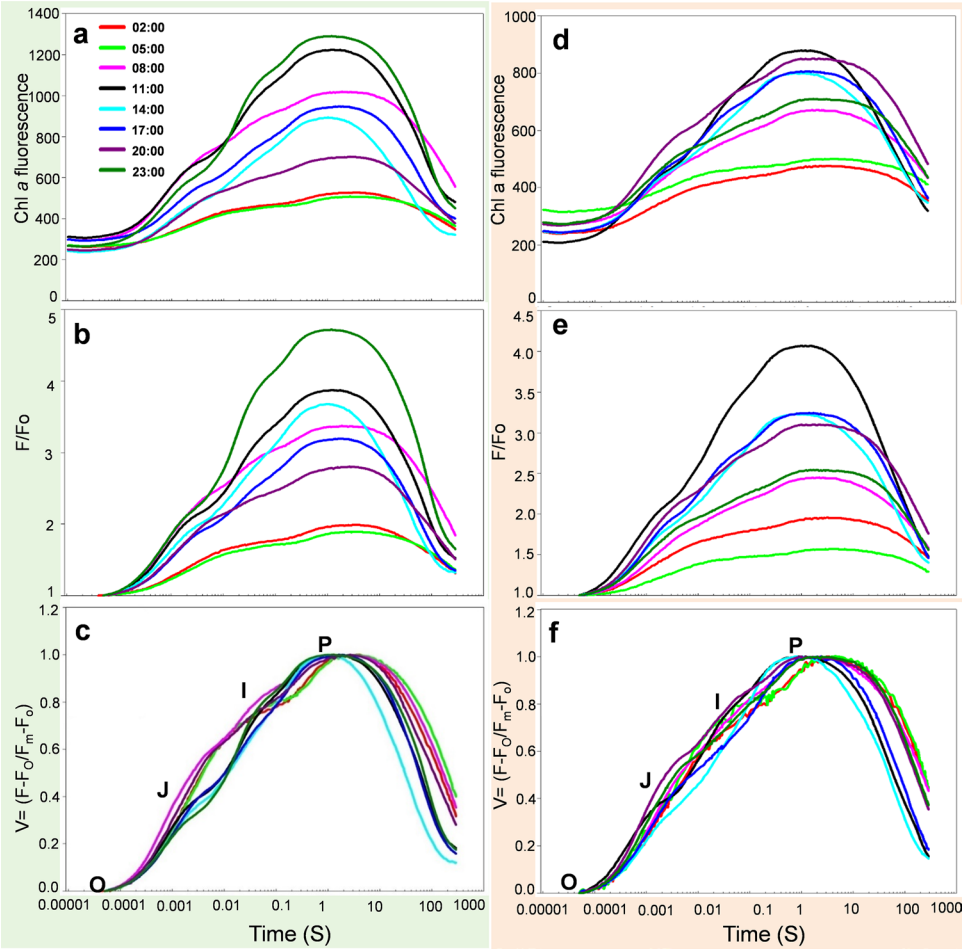

Fig. 3 Polyphasic OJIP transient rise for *Suaeda fruticosa* under diurnal or continuous dark condition. For each time point, the relative variable fluorescence was measured for 300 s and the data obtained were plotted on a log scale. The right panel shows the OJIP curve obtained from the plant that is under diurnal condition. The left panel is for the plant that is under continuous dark condition. **a**, **d** The raw Chl *a* fluorescence obtained at different time points, **b**, **e** fluorescence curves obtained after normalizing at O level (F_o), and **c**, **f** variable fluorescence (V) at time t obtained after normalizing at O and P (F_o and F_m) levels

as well as continuous dark conditions showed comparable significant changes unlike the parameters obtained from the gas exchange data, using IRGA, wherein the measured parameters showed lower amplitude during continuous dark (Supplementary Fig. S5).

The OJIP fluorescence rise under diurnal and continuous dark conditions

To compare the OJIP fluorescence rise between plants under diurnal and continuous dark (Fig. 3), single normalized (at F_o) fluorescence induction curves (i.e., F/F_o) were calculated for both conditions at each time point (see Fig. 4) and plotted from 0 to 300 s on a logarithmic time scale. Differences were observed in the pattern of the polyphasic OJIP fluorescence rise between the plant that was under diurnal from those under continuous dark at each time point. At 02:00 and 05:00 hrs, the fluorescence rise under both conditions shows slow fluorescence rise (Fig. 4a, b). From 08:00 hrs until 23:00 hrs, the OJIP rise under both the conditions increases (Fig. 4c–h). Under diurnal condition, the OJIP rise at 08:00, 14:00, and 23:00 hrs showed higher values than that under continuous dark. However, at 11:00 and 20:00 hrs, the OJIP rise was higher under continuous dark condition. Under both the conditions and at all the time points, maximum fluorescence rise was observed at 23:00 hrs under diurnal rhythm (Fig. 4h). Under continuous dark, maximum fluorescence was observed at 11:00 hrs (Fig. 4d). The increase in the OJIP rise corresponded to the increase in F_v/F_m, under both diurnal and continuous dark conditions.

To further compare the variable fluorescence between the plants under diurnal and continuous dark, the relative variable fluorescence, $V(t) = (F(t) - F_o)/(F_m - F_o)$, was calculated for both circadian rhythm and continuous dark condition at each time point (Supplementary Fig. S6). Differences were observed in the pattern of the polyphasic O–J–I–P transient rise between the plant that was under diurnal from those under continuous dark at each time point. However, under both the conditions, a distinct 'J' step was not observed during 02:00 and 05:00 hrs (Supplementary Fig. S6a, b). A high value of relative variable fluorescence between O–J fluorescence rise was observed during 08:00 and 20:00 hrs (Supplementary Fig. S6c, g) under both the conditions. In addition, under diurnal condition, distinct 'J' and 'I' steps

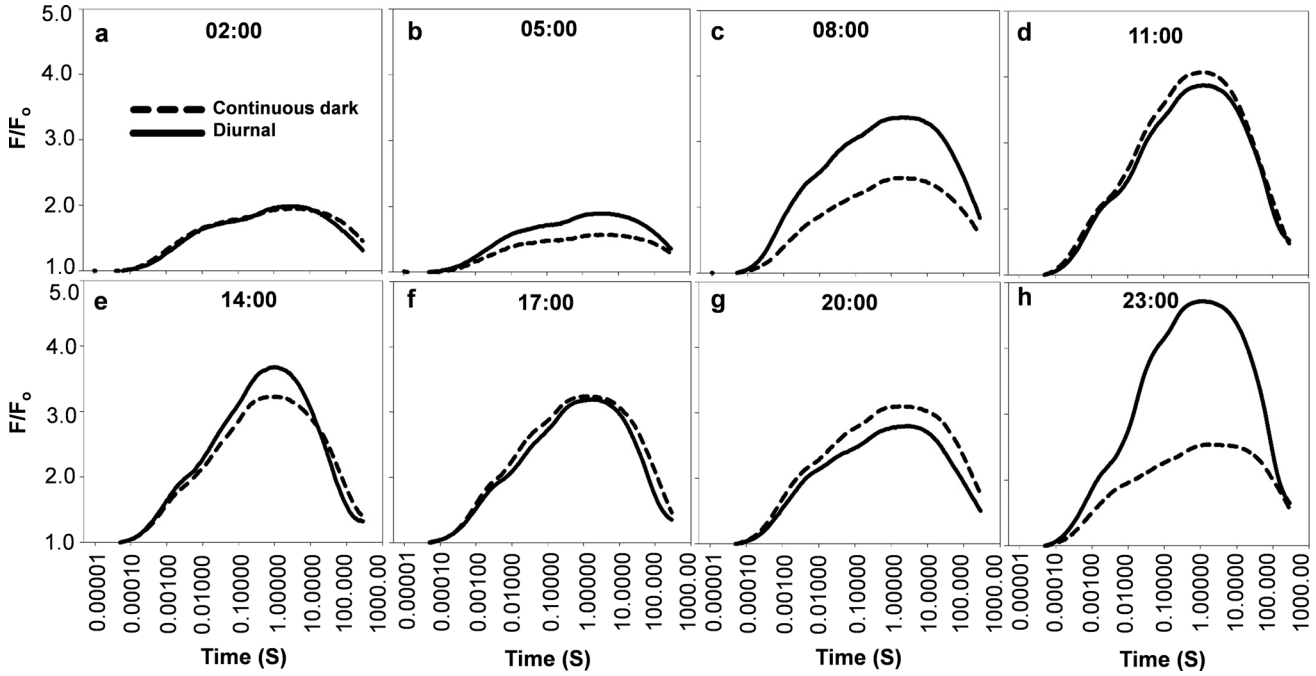

Fig. 4 Comparison of the OJIP fluorescence curves (normalized at F_o level) at different time points in the leaves of *Suaeda fruticosa* maintained under diurnal (full line) or continuous dark (broken line)

were observed during 23:00 hrs; however, the I step was not observed in plants kept under continuous dark condition (Supplementary Fig. S6h).

Photosynthetic parameters obtained from the OJIP transient by using the JIP test

The JIP parameters (Strasser et al. 2000, 2004), obtained after double normalization to F_o and F_m of the fluorescence induction curves of *S. fruticosa* (see "Materials and methods" section), were categorized as follows: technical fluorescence parameters, specific energy fluxes, phenomenological energy fluxes, and performance indices, as shown in Table 1 (see also, e.g., Bussotti et al. 2010; Stirbet and Govindjee 2011; Gururani et al. 2015; Marcińska et al. 2017). In this work, the calculated JIP parameters were represented in a heat map, by scaling them between 1 and 100 by using a color code in which green signifies low and red high values (Fig. 5); their respective values (in %) are also given in Supplementary Tables S1 and S2.

Under the diurnal rhythm (Fig. 5a), the time to attain maximum fluorescence (t_{Fm}) was at 14:00 hrs, while the minimum time to attain F_m was observed between 02:00 and 05:00 hrs. Similarly, under continuous dark condition (Fig. 5b), the lowest time to attain F_m was observed between 11:00 and 17:00 hrs, and the maximum time at 02:00 hrs. The maximum complementary area of the OJIP transient was found to be at 23:00 hrs under the diurnal rhythm, but at 20:00 hrs under continuous dark condition, while the minimum was obtained around 05:00 hrs in both cases. The slopes of the O–J rise (M_o), J–I phase (M_{JI}), and I–P phase (M_{IP}) were maximum around 08:00 hrs, 02:00 hrs, and 23:00 hrs, under diurnal condition (Fig. 5a). However, these three slopes were maximum around 20:00 hrs under continuous dark condition (Fig. 5b).

Our results on four parameters from the specific energy fluxes category are described below. The maximum absorbed photon flux per active PSII (ABS/RC) and the dissipated excitonic energy flux per PSII reaction center (DI_o/RC) were observed at 05:00 and in between 08:00 and 14:00 hrs, under the diurnal condition. However, under continuous dark condition, both these parameters were maximum at 05:00 hrs. On the other hand, the minimum values for ABS/RC and DI_o/RC were observed around 11:00 and 23:00 hrs, under the diurnal condition, but at 20:00 and 11:00 hrs, under the continuous dark condition. Furthermore, the maximum PSII trapping rate (TR_o/RC) and ETR through PSII (ET_o/RC) were observed at 23:00 hrs, under diurnal, and at 11:00 hrs, under continuous dark.

Our data on the four parameters of phenomenological fluxes defined at the level of F_o, i.e., the absorbed photon flux per PSII cross section at time zero (ABS/CS_o), dissipation of excitonic energy flux in the form of heat per PSII cross section at time zero (DI_o/CS_o), trapped energy flux at time zero (TR_o/CS_o), and electron transport flux per PSII cross section at time zero (ET_o/CS_o) (Fig. 5), gave the

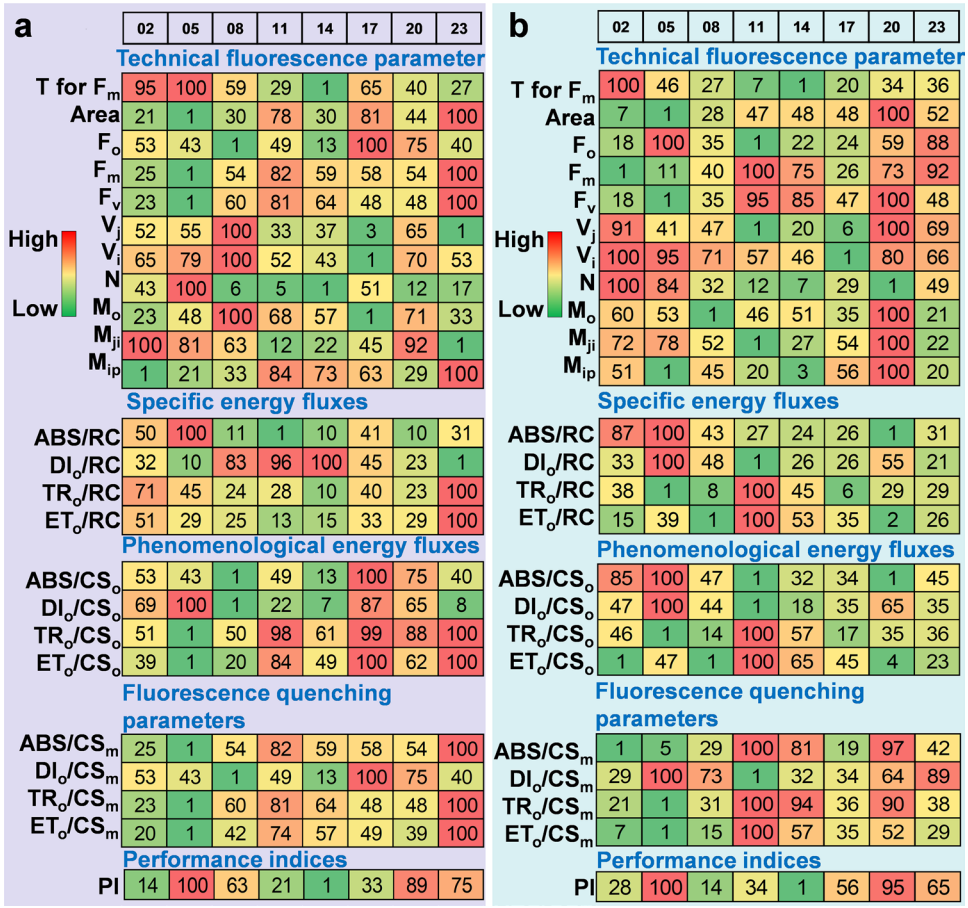

Fig. 5 Heat map representation of several photosynthesis-related parameters, obtained after using the JIP test for *Suaeda* under **a** diurnal and **b** continuous dark. Data are for different time points (02:00 to 23:00 hrs), obtained during 3 days (72 hrs). The plant under continuous dark was kept under diurnal condition for the first 24 hrs, followed by dark for 48 hrs where darkness was ensured by completely covering the plant with a dark cloth. Heat map of the parameters are shown in the figure: red is for high (100%), yellow for medium (50%), and green for the lowest values (1%). All the data obtained were first normalized to bring the value of the parameters in the range of 1–100 to provide an unbiased color code. Abbreviation and terminology of the parameters are given in Table 1

following result. All had the highest values around 17:00 hrs under the diurnal condition; however, under continuous dark condition, the maximum flux for both ABS/CS_o and DI_o/CS_o was at 05:00 hrs, while for both TR_o/CS_o and ET_o/CS_o, it was at 11:00 hrs. In addition, the absorbed photon flux per PSII cross section at F_m (ABS/CS_m), excitation energy trapped per PSII cross section at F_m (TR_o/CS_m), and ETR per PSII cross section at F_m (ET_o/CS_m) were maximum at 23:00 hrs under diurnal and 11:00 hrs, under continuous dark. In contrast, the energy dissipated per PSII cross section at F_m (DI_o/CS_m) was found to be maximum around 17:00 hrs, under diurnal and at 05:00 hrs, under continuous dark. Further, the overall performance index (PI_{total}) of *S. fruticosa* was found to be maximum at around 05:00 and at 20:00 hrs, while the minimum was at 14:00 hrs, under both conditions.

Discussion

In the hyper-saline inland playa located in the middle of the Aravalli schists within the Thar Desert of western India, roots of *S. fruticosa* are continuously exposed to highly saline soil (electrical conductivity, EC ranging from 45 to 50 dS m^{-1}), while their shoots are exposed to extremely hot (~ 50 °C during summer) and dry atmosphere (Krishna et al. 2014; Roy and Singhvi 2016; Sinha and Raymahashay 2004). Photosynthesis is the primary physiological process leading to growth and life of plants, and xerohalophytic *S. fruticosa* plants possess a wide range of specialized adaptation mechanisms to protect their photosynthetic apparatus under these extreme saline conditions (Wungrampha et al. 2018). The daily fluctuation in the temperature (from ~ 30 to 50 °C during the summer) and the high light intensity (1800 µmol photons m^{-2} s^{-1}) make it imperative for plants to adjust their photosynthesis machinery with the changes in these environmental conditions. Studies have been done in the past showing the existence of diurnal rhythm in the physiology of many plant species with respect to their photosynthesis (de Dios 2017; Matthews et al. 2017; Singh et al. 2015; Vialet-Chabrand et al. 2017). However, the present study is a unique attempt to study detailed photosynthesis parameters in a xero-halophyte growing around a salt lake, as affected by the diurnal rhythm and under dark conditions. Attempts have also been made in this study to identify and to examine the photosynthesis components associated with the complex adaptive processes in *S. fruticosa* under diurnal rhythm and under continuous dark conditions. Results, obtained in this study, support our hypothesis that the

photosynthetic activity of *S. fruticosa* is tightly regulated, which not only helps in its growth and development, but also in its adaptation to extreme environmental conditions.

Gas exchange and photosynthetic machinery is tightly regulated by the photoperiodic entrainment in *Suaeda fruticosa*

Photoperiodism in plants is a critical process that regulates the physiological behavior and its responsiveness under changing environmental conditions (Bendix et al. 2015; Moraes et al. 2019). In the present study, we have measured in situ gaseous exchange and the photosynthesis parameters of *S. fruticosa* under diurnal rhythm, as well as under continuous dark conditions. Under both conditions, the gaseous exchange and the photosynthetic parameters of *S. fruticosa* followed a rhythmic cycle repeated after every 24 hrs. However, under continuous dark conditions, the amplitudes of the measured parameters (such as G_s, NPQ, q_P, q_N, and C_i) were observed to be lower as compared to that under diurnal rhythm (Figs. 1, 2). Some of the parameters calculated in this study, such as G_s, NPR, q_P, and q_N, showed similar rhythmic pattern under both diurnal and continuous dark conditions. On the other hand, other parameters, such as C_i, NPQ, ETR, T_r, and F_v/F_m, showed reverse rhythmic pattern under continuous dark (Supplementary Fig. S4). Vialet-Chabrand et al. (2017) showed that the leaves of *Arabidopsis thaliana*, grown under fluctuating light and low light, are thinner, but the photosynthesis rate per unit area remains the same as that under diurnal conditions. However, we observe here that the rate of photosynthesis decreases in *S. fruticosa* under dark conditions.

Under diurnal conditions, parameters (arbitrarily called set 'A') such as the maximum quantum yield of PSII (F_v/F_m), stomatal conductance (G_s), and photochemical quenching (q_P) were found to be maximum at dawn, i.e., 05:00 hrs, and remained low during the rest of the day. This could be an adaptive feature for avoiding irreversible photodamage during high PAR and atmospheric temperature. In contrast, with the increase in PAR and temperature (from 08:00 to 17:00 hrs), parameters (arbitrarily called set 'B'), such as non-photochemical quenching (NPQ), intercellular CO_2 concentration (C_i), NPR, non-photochemical quenching coefficient (q_N), electron transport rate through PSII (ETR), and transpiration rate (T_r) (Figs. 1, 2), increased and showed a reverse pattern with the set 'A' parameters. However, within the set 'B' parameters, C_i and q_N showed another peak during 23:00 hrs but the amplitude of this peak was roughly half of that observed during light (around 14:00 hrs) (Fig. 2a, i). Interestingly, q_P stands out among all the parameters, as it was found to have a peak at dawn and another one at dusk, i.e., at 05:00 and 20:00 hrs (Fig. 2g).

Biomass and yield of a plant are directly proportional to the rate of photosynthesis (Zhu et al. 2008). Abiotic stress, such as salinity, directly affects the photosynthesis machinery of the plants, by damaging the photosynthesis pigments such as Chl, thus leading to a severe reduction of photosynthesis (Allakhverdiev et al. 2002; Wungrampha et al. 2018). In *S. fruticosa*, NPR and ETR were observed to be tightly regulated even under highly saline environment wherein maximum NPR was observed at 08:00 hrs under diurnal and 05:00 hrs during continuous dark (Fig. 1). As the light intensity and temperature increases during the day, NPR gradually declines which could be due to protection of the photosynthetic pigments under high light and temperature (Taylor and Rowley 1971).

Plants such as *A. thaliana*, *Phaseolus vulgaris*, *Vicia faba*, *Triticum aestivum*, and *Nicotiana tabacum*, under stable environment, balance the gain in carbon and water loss by tightly regulating NPR and G_s. However, the correlation between them varies depending on the availability of water since G_s also regulates net transpiration (T_r) in plants (Matthews et al. 2017). For instance, under long periods of drought leading to carbon starvation, plants reduce the rate of T_r by suppressing G_s rather than increasing the NPR to prevent water loss (Hills et al. 2012). Apart from this environmental factor, the role of photoperiodic regulation affecting the synchronic response of G_s and NPR is now emerging as a supplementary mechanism in plants to regulate carbon flux and water loss (de Dios 2017). However, the photoperiodic regulations for both G_s and NPR are different and are mutually independent of each other (Dodd et al. 2014). In *S. fruticosa*, G_s and NPR were found to be correlated under both diurnal rhythm (Fig. 1b, f) and under continuous dark (Fig. 2a, f); however, the net T_r and C_i varied under both the conditions.

de Dios (2017) has shown that 30% and 70% of the gas exchange in *Gossypium* sp. and members of the family *Fabaceae* are controlled by photoperiodic cycle. Additionally, in cotton and beans, the photoperiodic "memory" of the previous day regulates the gas exchange parameter irrespective of the environmental conditions (de Dios et al. 2016). However, in *S. fruticosa*, a similar effect of the 'previous day memory' was not observed in parameters such as C_i, NPQ, ETR, T_r, and F_v/F_m, which showed a reverse pattern under continuous dark (Figs. 1, 2). This could be due to its plasticity to adapt quickly under a changing environment.

Glycophytes such as *Arabidopsis* (Stepien and Johnson 2009), rice (Soda et al. 2018), barley, sorghum (Sharma and Hall 1991), and maize (Guo et al. 2017) respond to salinity by closing their stomata followed by a reduction in C_i, G_s, F_v/F_m, NPR, and ETR (Huang et al. 2016; Hwang and Choo 2016; Schuback et al. 2016). However, halophytes such as *Cakile* sp. (Megdiche et al. 2008), *Artemisia anethifolia* (Wen et al. 2005), *Suaeda salsa* (Wang et al. 2004), *Odyssea*

paucinervis (Naidoo et al. 2008), and *Paspalum vaginatum* (Lee et al. 2004) do not show significant changes in these parameters even though growth and biomass are compromised to a certain extent (Megdiche et al. 2008; Stepien and Johnson 2009). Likewise, *S. fruticosa* also showed routine cyclic pattern in these parameters representing acute adaptation under salinity stress.

Non-photochemical and photochemical quenching are regulated by light intensity

Under natural conditions, excess light intensity during midday leads to the production of ROS such as superoxide ($O_2^{\bullet-}$) and hydrogen peroxide (H_2O_2), resulting in photo-oxidative damage (Roach et al. 2015). It is interesting to know how certain organisms such as *Chlamydomonas*, *Chlorella* (Roach et al. 2015), *Erythrophleum*, *Khaya* (Huang et al. 2016), Ginkgo (Yang and Chen 2015), *Z. mays* (Leakey et al. 2004), *V. vinifera* (Downton et al. 1987), and phytoplankton (Schuback et al. 2016) protect their photosynthetic machinery by regulating the electron transport chain of their photosynthesis. One possible approach to do so is by operating reversible NPQ reaction coupled with q_P reaction or under the extreme case, through irreversible NPQ reaction (photoinhibition) (Stepien and Johnson 2009). In plants such as rice, during high light intensity, NPQ acts as a major photoprotective mechanism for their survival (Hamdani et al. 2019). The two parameters, i.e. NPQ and q_P, occur in reverse order wherein an increase of NPQ is followed by a decrease in q_P and vice versa (Huang et al. 2016). Increase in NPQ can broadly be due to two reasons: high-energy state quenching with the release of heat or due to photoinhibition (irreversible photosystem damage) (Stepien and Johnson 2009). In our study, we observed an increase of NPQ level in *S. fruticosa* at midday (Fig. 1e) followed by reduction in q_P. This could be due to the increase in PAR, after 11:00 hrs until 16:00 hrs (above 1500 µmol photons m^{-2} s^{-1}). This tight regulation of the NPQ and q_P to protect the photosynthesis machinery against high PAR might contribute to its adaptation under the combination of high temperature and salinity stress during the noon.

Furthermore, in *S. fruticosa* we observed an increase of F_v/F_m during dawn and dusk. This could be due to its ability for effective processing of light during low light intensities. The decrease in F_v/F_m from 08:00 hrs until 17:00 hrs suggests photoprotection of the PSII by reversible inactivation or down regulation during high light intensity, rather than photodamage. It is known that plants maintain higher photosynthesis rate and photochemical quenching during early morning hours when there is low radiation and high enzymatic activity of CO_2 assimilation cycle (Stepien and Johnson 2009). This observation further correlates with higher ETR, gas exchange, and transpiration rate during early morning hours. Since the midday depression in q_P was accompanied by enhanced C_i, it could be attributed to decreased photosynthetic activity of mesophyll cells, rather than the stomatal closure (Yang and Chen 2015). These mechanisms protect the photosystems of the plant from photooxidation by dissipating the excess energy as heat and also by maintaining a low steady-state fluorescence yield of PSII (Hajiboland 2014).

Furthermore, within a span of 24 hrs, under diurnal conditions, maximum F_v/F_m and NPR were observed between 20:00 and 05:00 hrs (in the absence of light) and at 08:00 hrs (Fig. 1a, c). However, under continuous dark, the quantum yield of PSII (as reflected by F_v/F_m) showed a gradual increase after dusk, attaining its maximum 2 hrs after noon (14:00 hrs) (Supplementary Fig. S5i), which is a reverse pattern to that under diurnal conditions. This result gives us an alternative perspective in addition to the photoprotective mechanism of PSII and, that is, *S. fruticosa* has a quick and systemic mechanism of repairing PSII that operates as PAR reduces (in the night, when there is no light). This might further help in reviving the PSIIs that were damaged during high light. The repair of the D1 protein of PSII during the night/low light has been reported in several photosynthetic organisms such as diatoms (Li et al. 2016), *Arabidopsis* (Järvi et al. 2015), and spinach (Suorsa et al. 2014). Further, the increase in the PSII quantum yield during noon under the absence of light brings a new perspective of the inner clock (circadian) regulating the photosynthesis machinery in *S. fruticosa*. However, this further needs to be explored by analyzing the circadian regulation mechanism in this plant.

Alternative electron transport pathways regulate the carbon sink in *Suaeda fruticosa* during exposure to high light intensity

When the halophyte *Thellungiella* is subjected to salinity above 500 mM, there is a marginal inhibition in gas exchange, with a significant increase in electron flow involving PSII (Stepien and Johnson 2009). This was found to be due to an increased activity of the terminal oxidase in plastids that acts as an alternative electron sink. This additional electron flow accounts to ~ 30% of the total ETR observed in plants under stress (Joët et al. 2002; Stepien and Johnson 2009). In *S. fruticosa*, G_s was seen to be lowest at the time when ETR was highest, i.e., between 05:00 and 14:00 hrs (Figs. 1e, 2c). The increase in total ETR when stomatal conductivity (G_s) is lower could be due to the activity of plastid terminal oxidase under the combination of both high temperature and salinity stress. Additionally, the observed increase in ETR at 05:00 hrs (even though the complementary area of the OJIP transient is the lowest) could be due to chlororespiration, involving both non-photochemical reduction as well as oxidation of PQ during the induction

of photosynthesis during the course of dark-to-light transition (Joët et al. 2002). The midday depression of q_P, which was accompanied by enhanced C_i, could be correlated with the decrease in the photosynthetic activity of the mesophyll cells, rather than the stomatal closure, such as that of *Ginkgo biloba* (Yang and Chen 2015). These mechanisms further protect photosystems from photooxidation by dissipating the excess energy as heat and also by maintaining a low steady-state fluorescence yield of PSII (Hajiboland 2014).

Chlorophyll *a* fluorescence follows rhythmic cycle under both diurnal and constant dark conditions in *Suaeda fruticosa*

The fast (within a second) OJIP polyphasic Chl *a* fluorescence rise (Strasser et al. 2004) at the beginning of the Chl *a* fluorescence induction transient is known to be influenced by environmental changes and the physiological state of the plant (Luo et al. 2016), since PSII is often the primary target under stress (Gururani et al. 2015; Soda et al. 2018). Under salinity (Lee et al. 2004; Soda et al. 2018), high temperature (Allakhverdiev et al. 2008; Mathur et al. 2011), drought (Luo et al. 2016) and change in light intensity during diurnal condition (Bacarin et al. 2016), changes in the value of F_o, time to reach F_m (t_{Fm}), complementary area of the OJIP curve, and other JIP parameters have been reported in several photosynthetic organisms. The analysis of the OJIP transient over the years has broadened our understanding of the function of PSII under many different conditions (cf. Stirbet et al. 2018). The so-called JIP test has been very useful for the analysis of the PSII activity (e.g., Luo et al. 2016; Stirbet and Govindjee 2011).

Our aim was to use the OJIP transient, as well as parameters defined in the JIP test, to investigate the effect of photoperiods (under diurnal rhythm and continuous darkness) on PSII activity of *S. fruticosa*, which thrives in a high saline environment. By calculating the JIP parameters (cf. Table 1), we observed a decline of the I–P phase and the complementary area of the OJIP curve during the day (Fig. 5). This might be due to the acclimation response of *S. fruticosa* to tolerate high PAR under prevailing salinity to maintain the redox poise of the PQ pool. It has been reported that the hindrance of the electron flow, either due to stress or any other factors, leads to drastic reduction in the complementary area of the OJIP curve (see, e.g., Gautam et al. 2014). Furthermore, the rapid recovery of photodamaged PSII is dependent on PSI activity as the stabilization of PSI activity during the daytime has been shown to contribute towards photoprotection and recovery of PSII activity (Huang et al. 2016). Thus, our study suggests that *S. fruticosa* stabilizes PSII complex proteins and prevents the disruption of electron transport to the PQ pool under high saline conditions.

Under circadian rhythm (by maintaining constant light), *Gonyaulax polyedra* was shown to display faster OJIP rise as compared to that under diurnal rhythm (Govindjee et al. 1979). The same phenomenon was also observed here in *S. fruticosa* under constant dark wherein, at all the time points, the time taken to attain F_m was faster under continuous dark condition (Fig. 5). Changes in energy fluxes per PSII reaction center are specific functional parameters, while the energy fluxes per excited cross section correspond to phenomenological energy fluxes (Gururani et al. 2015). Thus, by analyzing Chl *a* fluorescence transient, the energy flow cascade through electron transport chain can be determined (see, e.g., Bacarin et al. 2016). In this work, we observed high amount of energy dissipated in the form of heat from a PSII reaction center (DI_o/RC) during the daytime; this was further followed by decreased energy trapping at the reaction center (TR_o/RC). In contrast, and as expected, under low light intensities, most of the light absorbed by the Chl is utilized in photochemical reactions.

PSII is known to be much more susceptible to high temperatures as compared to PSI, since it inhibits the water oxidation complex (see, e.g., Bacarin et al. 2016; Nash et al. 1985). Indeed, a decrease in electron transport to the PQ pool (ET_o/RC) and in the antenna size of an active PSII reaction center (ABS/RC) was observed in this study (Fig. 5) during noon. These studies show that under high light intensity (i.e., during daytime) *S. fruticosa* regulates the total electron flux by decreasing the size of the antenna in PSII. The increase in DI_o/RC further confirms that excess absorbed light is dissipated primarily through reaction centers as well as antenna during the daytime leading to a decrease in photochemical reactions. Changes in PI_{total} were shown to follow the pattern of F_v/F_m with similar amplitude, indicating a similar sensitivity of PI_{total} to changes in light and temperature in this plant. Previous studies on different halophytes such as *A. anethifolia* (Lu et al. 2003; Wen et al. 2005), *S. salsa* (Wang et al. 2004), *P. vaginatum* (Lee et al. 2004), *Cakile maritima* (Megdiche et al. 2008), *Porteresia coarctata* (Sengupta and Majumder 2009), *Aster tripolium* (*Duarte* et al. 2017), *O. paucinervis* (Naidoo et al. 2008), and *Thellungiella salsuginea* (Goussi et al. 2018) have also demonstrated that these plants maintain their phenomenological energy flux even under salinity. Similarly, it had been shown earlier that circadian oscillations contribute towards the regulation of light harvesting from the photosynthetic apparatus at both transcriptional and post-translational levels (Dodd et al. 2014; Locke et al. 2018). It is highly likely that this may be due to the accumulation of osmolytes and soluble compounds such as sugars and proteins that help in stabilizing the oxygen-evolving complex and PSII core from salinity stress. In our previous study (Singh et al. 2015; Nongpiur et al. 2019), we have shown that expression of genes such as *Prr*, *HK*s, *Hpt*s, and *RR* of the 'two-component system' gene family regulates

the circadian clock in rice seedlings under different abiotic stress conditions, thus unraveling an alternate transcriptional control mechanism in higher plants.

Conclusion

The present study compares in situ Chl fluorescence kinetics of *S. fruticosa* in diurnal and constant dark conditions under extreme saline conditions. In our previous studies (Soda et al. 2018) on glycophytes, we had reported that salinity stress severely influences PSI and PSII activities as well as Chl *a* fluorescence. The work presented here is the first study demonstrating that the prime strategy enabling the halophyte *S. fruticosa* to grow in extremely saline environment is to maintain structural integrity and electron flow through PSI and PSII along with the protection of photosynthesis machinery from photoinhibition during high irradiance at midday. Moreover, Chl *a* fluorescence parameter revealed that midday depression in photosynthesis and photochemical activity of PSII in *S. fruticosa* enables the maintenance of the equilibrium of electron flow from the antenna complex to PSII reaction center and CO_2 gas exchange in the fluctuating microclimate. Further, metabolic fingerprinting and proteomic analysis of *S. fruticosa* under the influence of diurnal condition are planned for future studies to help us untangle the complex adaptive machinery of this halophyte, which enables it to survive under severe environmental conditions.

Acknowledgements SW, RJ, and RSR acknowledge Senior Research Fellowship from UGC (University Grants Commission, Government of India), Dr. D. S. Kothari Postdoctoral Fellowship from UGC, and DST-Inspire Doctoral Fellowship from DST (Department of Science and Technology), Government of India. Research in the Lab of AP is supported by funding from the Indo-US Science and Technology Forum (IUSSTF) for Indo-US Advanced Bioenergy Consortium (IUABC), International Atomic Energy Agency (Vienna), and UPE-II (India). Govindjee thanks the Departments of Plant Biology and Biochemistry of the University of Illinois at Urbana-Champaign for the use of computer facilities and office space. We thank Alexendrina Stirbet for reading this manuscript, especially Table 1.

Authors contribution SW, RJ, and RSR carried out the experiments. SW and RJ drafted the manuscript. AP conceived and designed the study. AP, SLS-P, and G finalized the manuscript. All the authors have read and approved the final manuscript.

Compliance with ethical standards

Conflict of interest The authors declare that they have no conflict of interest.

References

Allakhverdiev SI, Sakamoto A, Nishiyama Y, Inaba M, Murata N (2000) Ionic and osmotic effects of NaCl-induced inactivation of photosystems I and II in *Synechococcus* sp. Plant Physiol 123(3):1047–1056

Allakhverdiev SI, Nishiyama Y, Miyairi S, Yamamoto H, Inagaki N, Kanesaki Y, Murata N (2002) Salt stress inhibits the repair of photodamaged photosystem II by suppressing the transcription and translation of psbA genes in *Synechocystis*. Plant Physiol 130(3):1443–1453

Allakhverdiev SI, Kreslavski VD, Klimov VV, Los DA, Carpentier R, Mohanty P (2008) Heat stress: an overview of molecular responses in photosynthesis. Photosynth Res 98(1–3):541

Bacarin MA, Martinazzo EG, Cassol D, Falqueto AR, Silva DM (2016) Daytime variations of chlorophyll *a* fluorescence in Pau D'alho seedlings. Rev Árvore 40(6):1023–1030

Bahn M, Schmitt M, Siegwolf R, Richter A, Bruggemann N (2009) Does photosynthesis affect grassland soil-respired CO_2 and its carbon isotope composition on a diurnal time scale? N Phytol 182(2):451–460

Bastías E, González-Moro MB, González-Murua C (2015) Interactive effects of excess boron and salinity on response curves of gas exchange to increase in the intensity of light of *Zea mays* amylacea from the Lluta Valley (Arica-Chile). IDESIA (Chile) 33:33–38

Bendix C, Marshall CM, Harmon FG (2015) Circadian clock genes universally control key agricultural traits. Mol Plant 8(8):1135–1152

Bussotti F, Desotgiu R, Pollastrini M, Cascio C (2010) The JIP test: a tool to screen the capacity of plant adaptation to climate change. Scand J For Res 25(S8):43–50

Cano-Ramirez DL, Dodd AN (2018) New connections between circadian rhythms, photosynthesis, and environmental adaptation. Plant Cell Environ 41(11):2515–2517

Chen TW, Stützel H, Kahlen K (2017) High light aggravates functional limitations of cucumber canopy photosynthesis under salinity. Ann Bot 121(5):797–807

Cheng T, Zhang G, Zhang S, Al Z, Zhang Y (2016) Photosynthesis diurnal variation of *Xanthoceras sorbifolia* Bunge under different soil water conditions. Acta Bot Sin 9:16

De Caluwé J, de Melo JRF, Tosenberger A, Hermans C, Verbruggen N, Leloup JC, Gonze D (2017) Modeling the photoperiodic entrainment of the plant circadian clock. J Theor Biol 420:220–231

de Dios VR (2017) Circadian regulation and diurnal variation in gas exchange. Plant Physiol 175(1):3–4

de Dios VR, Gessler A, Ferrio JP, Alday JG, Bahn M, del Castillo J, Devidal S, García-Muñoz S, Kayler Z, Landais D, Martín-Gómez P, Milcu A, Piel C, Pirhofer-Walzl K, Ravel O, Salekin S, Tissue DT, Tjoelker MG, Voltas J, Roy J (2016) Circadian rhythms have significant effects on leaf-to-canopy scale gas exchange under field conditions. GigaScience 5:43

Dodd AN, Kusakina J, Hall A, Gould PD, Hanaoka M (2014) The circadian regulation of photosynthesis. Photosynth Res 119(1–2):181–190

Downton WJS, Grant WJR, Loveys BR (1987) Diurnal changes in the photosynthesis of field-grown grape vines. N Phytol 105(1):71–80

Duarte B, Cabrita MT, Gameiro C, Matos AR, Godinho R, Marques JC, Cacador I (2017) Disentangling the photochemical salinity tolerance in *Aster tripolium* L.: connecting biophysical traits with changes in fatty acid composition. Plant Biol 19(2):239–248

Epron D, Dreyer E, Breda N (1992) Photosynthesis of oak trees [*Quercus petraea* (Matt.) Liebl.] during drought under field conditions: diurnal course of net CO_2 assimilation and photochemical efficiency of photosystem II. Plant Cell Environ 15(7):809–820

Feng D, Wang Y, Lu T, Zhang Z, Han X (2017) Proteomics analysis reveals a dynamic diurnal pattern of photosynthesis-related pathways in maize leaves. PLoS ONE 12(7):e0180670

Fisher RA (ed) (2006) Statistical methods for research workers. Genesis Publishing Pvt. Ltd., New Delhi

Flowers TJ, Colmer TD (2015) Plant salt tolerance: adaptations in halophytes. Ann Bot 115(3):327–331

García-Plazaola JI, Fernández-Marín B, Ferrio JP, Alday JG, Hoch G, Landais D, Milcu A, Tissue DT, Voltas J, Gessler A, Roy J, de Dios VR (2017) Endogenous circadian rhythms in pigment composition induce changes in photochemical efficiency in plant canopies. Plant Cell Environ 40(7):1153–1162

Gautam A, Agrawal D, SaiPrasad SV, Jajoo A (2014) A quick method to screen high and low yielding wheat cultivars exposed to high temperature. Physiol Mol Biol Plant 20(4):533–537

Goldstein A, Annor G, Vamadevan V, Tetlow I, Kirkensgaard JJ, Mortensen K, Blennow A, Hebelstrup KH, Bertoft E (2017) Influence of diurnal photosynthetic activity on the morphology, structure, and thermal properties of normal and waxy barley starch. Int J Biol Macromol 98:188–200

Goussi R, Manaa A, Derbali W, Cantamessa S, Abdelly C, Barbato R (2018) Comparative analysis of salt stress, duration and intensity, on the chloroplast ultrastructure and photosynthetic apparatus in *Thellungiella salsuginea*. J Photochem Photobiol B 183:275–287

Govindjee, Wong D, Prézelin BB, Sweeney BM (1979) Chlorophyll *a* fluorescence of *Gonyaulax polyedra* grown on a light–dark cycle and after transfer to constant light. Photochem Photobiol 30(3):405–411

Greenham K, McClung CR (2015) Integrating circadian dynamics with physiological processes in plants. Nat Rev Genet 16(10):598

Guo R, Shi L, Yan C, Zhong X, Gu F, Liu Q, Xia X, Li H (2017) Ionomic and metabolic responses to neutral salt or alkaline salt stresses in maize (*Zea mays* L.) seedlings. BMC Plant Biol 17(1):41

Gururani MA, Venkatesh J, Ganesan M, Strasser RJ, Han Y, Kim JI, Lee HY, Song PS (2015) In vivo assessment of cold tolerance through chlorophyll-*a* fluorescence in transgenic Zoysiagrass expressing mutant phytochrome A. PLoS ONE 10(5):e0127200

Hajiboland R (2014) Reactive oxygen species and photosynthesis. In: Ahmad P (ed) Oxidative damage to plants: antioxidant networks and signaling. Academic, Cambridge, pp 1–63

Hamdani S, Khan N, Perveen S, Qu M, Jiang J, Zhu XG (2019) Changes in the photosynthesis properties and photoprotection capacity in rice (*Oryza sativa*) grown under red, blue, or white light. Photosynth Res 139(1–3):107–121

Hills A, Chen ZH, Amtmann A, Blatt MR, Lew VL (2012) On Guard, a computational platform for quantitative kinetic modeling of guard cell physiology. Plant Physiol 159:1026–1042

Huang W, Yang YJ, Hu H, Cao KF, Zhang SB (2016) Sustained diurnal stimulation of cyclic electron flow in two tropical tree species *Erythrophleum guineense* and *Khaya ivorensis*. Front Plant Sci 7:1068

Hwang JS, Choo YS (2016) Solute patterns and diurnal variation of photosynthesis and chlorophyll fluorescence in Korean coastal sand dune plants. Photosynthetica 55(1):107–120

Ikkonen EN, Shibaeva TG, Rosenqvist E, Ottosen CO (2015) Daily temperature drop prevents inhibition of photosynthesis in tomato plants under continuous light. Photosynthetica 53(3):389–394

Järvi S, Suorsa M, Aro EM (2015) Photosystem II repair in plant chloroplasts—regulation, assisting proteins and shared components with photosystem II biogenesis. BBA Bioenerg 1847(9):900–909

Joët T, Genty B, Josse EM, Kuntz M, Cournac L, Peltier G (2002) Involvement of a plastid terminal oxidase in plastoquinone oxidation as evidenced by expression of the *Arabidopsis thaliana* enzyme in tobacco. J Biol Chem 277(35):31623–31630

Joshi R, Karan R, Singla-Pareek SL, Pareek A (2016) Ectopic expression of Pokkali phosphoglycerate kinase-2 (*OsPGK2-P*) improves yield in tobacco plants under salinity stress. Plant Cell Rep 35(1):27–41

Kan X, Ren J, Chen T, Cui M, Li C, Zhou R, Zhang Y, Liu H, Deng D, Yin Z (2017) Effects of salinity on photosynthesis in maize probed by prompt fluorescence, delayed fluorescence and P700 signals. Environ Exp Bot 140:56–64

Kim SW, Lee SK, Jeong HJ, An G, Jeon JS, Jung KH (2017) Crosstalk between diurnal rhythm and water stress reveals an altered primary carbon flux into soluble sugars in drought-treated rice leaves. Sci Rep 7(1):8214

Kolosova N, Gorenstein N, Kish CM, Dudareva N (2001) Regulation of circadian methyl benzoate emission in diurnally and nocturnally emitting plants. Plant Cell 13(10):2333–2347

Krishna PH, Reddy CS, Meena SL, Katewa SS (2014) Pattern of plant species diversity in grasslands of Rajasthan, India. Taiwania 59(2):111–118

Kumar G, Kushwaha HR, Panjabi-Sabharwal V, Kumari S, Joshi R, Karan R, Mittal S, Pareek SLS, Pareek A (2012) Clustered metallothionein genes are co-regulated in rice and ectopic expression of *OsMT1e-P* confers multiple abiotic stress tolerance in tobacco via ROS scavenging. BMC Plant Biol 12(1):107

Lazár D (2015) Parameters of photosynthetic energy partitioning. J Plant Physiol 175:131–147

Leakey ADB, Bernacchi CJ, Dohleman FG, Ort DR, Long SP (2004) Will photosynthesis of maize (*Zea mays*) in the US corn belt increase in future [CO_2] rich atmospheres? An analysis of diurnal courses of CO_2 uptake under free-air concentration enrichment (FACE). Glob Change Biol 10(6):951–962

Lee G, Carrow RN, Duncan RR (2004) Photosynthetic responses to salinity stress of halophytic seashore paspalum ecotypes. Plant Sci 166(6):1417–1425

Li G, Woroch AD, Donaher NA, Cockshutt AM, Campbell DA (2016) A hard day's night: diatoms continue recycling photosystem II in the dark. Front Mar Sci 3:218

Locke AM, Slattery RA, Ort DR (2018) Field-grown soybean transcriptome shows diurnal patterns in photosynthesis-related processes. Plant Direct 2:1–14

Lu A, Jiang G, Wang B, Kuang T (2003) Photosystem II photochemistry and photosynthetic pigment composition in salt-adapted halophyte *Artemisia anethifolia* grown under outdoor conditions. J Plant Physiol 160:403–4008

Luo HH, Merope TM, Zhang YL, Zhang WF (2016) Combining gas exchange and chlorophyll *a* fluorescence measurements to analyze the photosynthetic activity of drip-irrigated cotton under different soil water deficits. J Integr Agric 15(6):1256–1266

Marcińska I, Czyczyło-Mysza I, Skrzypek E, Grzesiak MT, Popielarska-Konieczna M, Warchoł M, Grzesiak S (2017) Application of photochemical parameters and several indices based on phenotypical traits to assess intraspecific variation of oat (*Avena sativa* L.) tolerance to drought. Acta Physiol Plant 39(7):153

Mathur S, Jajoo A, Mehta P, Bharti S (2011) Analysis of elevated temperature-induced inhibition of photosystem II using chlorophyll *a* fluorescence induction kinetics in wheat leaves (*Triticum aestivum*). Plant Biol 13(1):1–6

Matthews JS, Vialet-Chabrand SR, Lawson T (2017) Diurnal variation in gas exchange: the balance between carbon fixation and water loss. Plant Physiol 174(2):614–623

McClung CR (2006) Plant circadian rhythms. Plant Cell 18(4):792–803

Megdiche W, Hessini K, Gharbi F, Jaleel CA, Ksouri R, Abdelly C (2008) Photosynthesis and photosystem 2 efficiency of two salt-adapted halophytic seashore *Cakile maritima* ecotypes. Photosynthetica 46(3):410–419

Meng F, Luo Q, Wang Q, Zhang X, Qi Z, Xu F, Lei X, Cao Y, Chow WS, Sun G (2016) Physiological and proteomic responses to salt stress in chloroplasts of diploid and tetraploid black locust (*Robinia pseudoacacia* L.). Sci Rep 6:23098

Mishra KB, Mishra A, Klem K, Govindjee (2016) Plant phenotyping: a perspective. Indian J Plant Physiol 21(4):514–527

Moraes TA, Mengin V, Annunziata MG, Encke B, Krohn N, Hoehne M, Stitt M (2019) Response of the circadian clock and diel starch turnover to one day of low light or low CO_2. Plant Physiol 179(4):1457–1478

Mora-García S, de Leone MJ, Yanovsky M (2017) Time to grow: circadian regulation of growth and metabolism in photosynthetic organisms. Curr Opin Plant Biol 35:84–90

Naidoo G, Somaru R, Achar P (2008) Morphological and physiological responses of the halophyte, *Odyssea paucinervis* (Staph) (Poaceae), to salinity. Flora 203(5):437–447

Nash D, Miyao M, Murata N (1985) Heat inactivation of oxygen evolution in Photosystem II particles and its acceleration by chloride depletion and exogenous manganese. Biochim Biophys Acta 807:127–133

Nitschke S, Cortleven A, Iven T, Feussner I, Havaux M, Riefler M, Schmülling T (2016) Circadian stress regimes affect the circadian clock and cause jasmonic acid-dependent cell death in cytokinin-deficient *Arabidopsis* plants. Plant Cell 28(7):1616–1639

Nongpiur RC, Singla-Pareek SL, Pareek A (2019) The quest for 'osmosensors' in plants. J Exp Bot. https://doi.org/10.1093/jxb/erz263

Pan WJ, Wang X, Deng YR, Li JH, Chen W, Chiang JY, Yang JB, Zheng L (2015) Nondestructive and intuitive determination of circadian chlorophyll rhythms in soybean leaves using multispectral imaging. Sci Rep 5:11108

Papageorgiou GC, Govindjee (eds) (2004) Chlorophyll *a* fluorescence: a signature of photosynthesis. Springer, Dordrecht

Pareek A, Sopory SK, Bohnert HJ, Govindjee (2010) Abiotic stress adaptation in plants: physiological, molecular and genomic foundation. Springer, Dordrecht

Roach T, Miller R, Aigner S, Kranner I (2015) Diurnal changes in the xanthophyll cycle pigments of freshwater algae correlate with the environmental hydrogen peroxide concentration rather than non-photochemical quenching. Ann Bot 116(4):519–527

Roy PD, Singhvi AK (2016) Climate variation in the Thar Desert since the last glacial maximum and evaluation of the Indian monsoon. TIP Rev Espec Cienc Quím-Biol 19(1):32–44

Saeed AI, Bhagabati NK, Braisted JC, Liang W, Sharov V, Howe EA, Li J, Thiagarajan M, White JA, Quackenbush J (2006) [9] TM4 microarray software suite. Method Enzymol 411:134–193

Schaffer R, Landgraf J, Accerbi M, Simon V, Larson M, Wisman E (2001) Microarray analysis of diurnal and circadian-regulated genes in *Arabidopsis*. Plant Cell 13:113–123

Schreiber U, Schliwa U, Bilger W (1986) Continuous recording of photochemical and non-photochemical chlorophyll fluorescence quenching with a new type of modulation fluorometer. Photosynth Res 10(1–2):51–62

Schuback N, Flecken M, Maldonado MT, Tortell PD (2016) Diurnal variation in the coupling of photosynthetic electron transport and carbon fixation in iron-limited phytoplankton in the NE Subarctic Pacific. Biogeosciences 13(4):1019–1035

Sengupta S, Majumder AL (2009) Insight into the salt tolerance factors of a wild halophytic rice, *Porteresia coarctata*: a physiological and proteomic approach. Planta 229(4):911–929

Sengupta S, Mangu V, Sanchez L, Bedre R, Joshi R, Rajasekaran K, Baisakh N (2018) An actin depolymerizing factor from the halophyte smooth cordgrass, *Spartina alterniflora* (*SaADF2*) is superior to its rice homolog (*OsADF2*) in conferring drought and salt tolerance when constitutively overexpressed in rice. Plant Biotechnol J 503(3):1516–1523

Sharan A, Soni P, Nongpiur RC, Singla-Pareek SL, Pareek A (2017) Mapping the 'Two-component system' network in rice. Sci Rep 7(1):9287

Sharma PK, Hall DO (1991) Interaction of salt stress and photoinhibition on photosynthesis in Barley and Sorghum. J Plant Physiol 138(5):614–619

Shor E, Green RM (2016) The impact of domestication on the circadian clock. Trends Plant Sci 21(4):281–283

Singh A, Kushwaha HR, Soni P, Gupta H, Singla-Pareek SL, Pareek A (2015) Tissue specific and abiotic stress regulated transcription of histidine kinases in plants is also influenced by diurnal rhythm. Front Plant Sci 6:711

Sinha R, Raymahashay BC (2004) Evaporite mineralogy and geochemical evolution of the Sambhar Salt Lake, Rajasthan, India. Sediment Geol 166(1–2):59–71

Soda N, Gupta BK, Anwar K, Sharan A, Govindjee, Singla-Pareek SL, Pareek A (2018) Rice intermediate filament, OsIF, stabilizes photosynthetic machinery and yield under salinity and heat stress. Sci Rep 8(1):4072

Soni P, Kumar G, Soda N, Singla-Pareek SL, Pareek A (2013) Salt overly sensitive pathway members are influenced by diurnal rhythm in rice. Plant Signal Behav 8(7):e24738

Stepien P, Johnson GN (2009) Contrasting responses of photosynthesis to salt stress in the glycophyte *Arabidopsis* and the halophyte *Thellungiella*: role of the plastid terminal oxidase as an alternative electron sink. Plant Physiol 149(2):1154–1165

Stirbet A, Govindjee (2011) On the relation between the Kautsky effect (chlorophyll *a* fluorescence induction) and Photosystem II: basics and applications of the OJIP fluorescence transient. J Photochem Photobiol B 104(1–2):236–257

Stirbet A, Govindjee (2012) Chlorophyll *a* fluorescence induction: a personal perspective of the thermal phase, the J–I–P rise. Photosynth Res 113(1–2):15–61

Stirbet A, Riznichenko GY, Rubin AB (2014) Modeling chlorophyll *a* fluorescence transient: relation to photosynthesis. Biochemistry (Mosc) 79(4):291–323

Stirbet A, Lazár D, Kromdijk J, Govindjee (2018) Chlorophyll *a* fluorescence induction: can just a one-second measurement be used to quantify abiotic stress responses? Photosynthetica 56(1):86–104

Strasser RJ (1978) The grouping model of plant photosynthesis. In: Akoyunoglou G, Argyroudi-Akoyunoglou JH (eds) Chloroplast development. Elsevier Biomedical, Amsterdam, pp 513–538

Strasser RJ, Srivastava A, Tsimilli-Michael M (2000) The fluorescence transient as a tool to characterize and screen photosynthetic samples. In: Strasser RJ, Srivastava A, Tsimilli-Michael M (eds) Probing photosynthesis: mechanisms, regulation and adaptation. Taylor and Francis, London, pp 445–483

Strasser RJ, Srivastava A, Tsimilli-Michael M (2004) Analysis of the chlorophyll *a* fluorescence transient. In: Papageorgiou GC, Govindjee (eds) Advances in photosynthesis and respiration chlorophyll fluorescence a signature of photosynthesis. Springer, Dordrecht, pp 321–362

Suorsa M, Rantala M, Danielsson R, Järvi S, Paakkarinen V, Schröder WP, Styring S, Mamedov F, Aro EM (2014) Dark-adapted spinach thylakoid protein heterogeneity offers insights into the photosystem II repair cycle. BBA Bioenerg 1837(9):1463–1471

Tang J, Baldocchi DD, Xu L (2005) Tree photosynthesis modulates soil respiration on a diurnal time scale. Glob Change Biol 11(8):1298–1304

Taylor AO, Rowley JA (1971) Plants under climatic stress: I. Low temperature, high light effects on photosynthesis. Plant Physiol 47(5):713–718

Ullah S, Bano A (2015) Physiological mechanism of salt tolerance in *Suaeda fruticosa* collected from high saline fields of Khyber Pukhtoon-Khwa, Pakistan. Commun Soil Sci Plant 46(10):1212–1228

Vialet-Chabrand S, Matthews JS, Simkin AJ, Raines CA, Lawson T (2017) Importance of fluctuations in light on plant photosynthetic acclimation. Plant Physiol 173(4):2163–2179

Wang B, Luttge U, Ratajczak R (2004) Specific regulation of SOD isoforms by NaCl and osmotic stress in leaves of the C_3 halophytes *Suaeda salsa* L. J Plant Physiol 161:285–293

Webb AA (2003) The physiology of circadian rhythms in plants. N Phytol 160(2):281–303

Wen X, Qiu N, Lu Q, Lu C (2005) Enhanced thermotolerance of photosystem II in salt-adapted plants of the halophyte *Artemisia anethifolia*. Planta 220(3):486–497

Wungrampha S, Joshi R, Singla-Pareek SL, Pareek A (2018) Photosynthesis and salinity: are these mutually exclusive? Photosynthetica 56(1):366–381

Yang XS, Chen GX (2015) Diurnal changes in gas exchange and chlorophyll fluorescence in *Ginkgo* leaves under field conditions. J Anim Plant Sci 25:309–313

Zhang RP, Yang DZ, Fu LS, Lu TG, Li DP, Xie FT (2007) Research of photosynthesis diurnal variation and its affecting factors for different source soybeans. Soybean Sci 26(4):490

Zhu XG, Long SP, Ort DR (2008) What is the maximum efficiency with which photosynthesis can convert solar energy into biomass? Curr Opin Biotechnol 19(2):153–159